

Moderating Virtual Reality Simulator Sickness by Changes in Brightness

Gizem Senel ¹, Ramon Oliva ², Maria V. Sanchez-Vives ³, Mel Slater ¹

¹ Event Lab, Department of Clinical Psychology and Psychobiology, Institute of Neurosciences of the University of Barcelona, University of Barcelona, Barcelona, Spain.

² Event Lab, Department of Clinical Psychology and Psychobiology, University of Barcelona, Barcelona, Spain

³ IDIBAPS, Barcelona, Spain

Abstract

The use of virtual reality is often uncomfortable since it induces simulator sickness. This especially occurs when there is a misalignment between vision and somatosensory and vestibular input – for example, where visual flow indicates movement through space, but in fact the body is stationary. Sensory conflict theory proposes that this is the prime cause of simulator sickness. Here we show that simulator sickness may be reduced through the exploitation of the ambient light of an environment. Participants move through a virtual street at a velocity determined by how much they depress a hand held controller. In experiment 1 they first moved through 4 street alternating street segments: either dark first, then bright, then dark, and then light, or alternating the same way but with the light street first. It was found that the mean velocity over the 2 dark streets and the 2 light streets, were not different. However, those who started in the dark street first maintained overall a greater velocity throughout and had less simulator sickness. We derived a statistical model that accounted for these results. In experiment 2 participants traversed a street that started out dark and gradually became bright, or a street that was bright throughout. The same statistical model was able to account for the results showing that the first exposure in a dark environment led to greater overall velocity and lower simulator sickness. This method suggests that in order to reduce the likelihood of simulator sickness in environments where traversal through the space plays a major role, that participants should start out in an environment that is dark which can gradually become brighter over time.

Keywords

Simulator sickness, virtual reality, ambient light, simulator sickness questionnaire, velocity

Introduction

Simulator sickness (cybersickness) is the bane of virtual reality (VR), perhaps a major reason why in spite of highly significant advances in the technology in recent years, and a dramatic fall in costs, it has still not taken off with consumers in a major way. If one's first experience of VR involves a significant degree of nausea and discomfort, it is unlikely that there will be

any great desire to try it again. This problem is heightened by the tendency to demonstrate VR to novices with exactly the types of scenarios most likely to cause simulator sickness – such as roller coaster rides where the optic flow indicates rapid movement but the body is stationary. The reference paper for simulator sickness, which introduced a widely used questionnaire (Kennedy et al., 1993), suggests that simulator sickness is signified by Nausea (N), Oculomotor Disturbance (O) and Disorientation (D). N consists of general discomfort, increased salivation, sweating, feelings of nausea, difficulty concentrating, stomach awareness and burping. O includes general discomfort, fatigue, headache, eyestrain, difficulty focusing, difficulty concentrating, and blurred vision. D includes difficulty focusing, feelings of nausea, fullness of head, blurred vision, dizziness with open or closed eyes, and vertigo. This questionnaire (the SSQ – simulator sickness questionnaire) has stood the test of time (Balk et al., 2013), although some caveats have been noted by Bimberg et al. (2020) in the context of its use for VR, especially regarding the use of the correct formula for computing final scores, and issues of interpretation. For more recent systematic review of the symptoms see (Davis et al., 2014).

Stanney and Kennedy (2009) provided an overview of simulator sickness where they pointed out that the most widely accepted cause is sensory conflict. Sensory Conflict Theory argues that simulator sickness is caused by discrepancies between the sensory inputs, where, for example, the optical flow indicates movement through space but the vestibular and somatosensory systems do not detect any corresponding physical movement. Hence this mismatch between the various signals can cause symptoms similar to motion sickness, such as nausea, dizziness, or disorientation. Sensory conflict theory is based on earlier work on motion sickness by Reason and Brand (1975) and was explored in relation to simulator sickness in virtual reality by Kolasinski (1995). The postural instability theory of simulator sickness (Riccio and Stoffregen, 1991) is an alternative to sensory conflict theory and originally developed to explain motion sickness. It suggests that the sickness may be caused by the inability of a person to control their posture in response to a conflicting sensory environment. The argument is that the difficulty to maintain balance and to control posture, rather than the sensory conflict itself, which may be caused by individual predisposition, leads to symptoms of simulator sickness. Warwick-Evans and Beaumont (1995) and Warwick-Evans et al. (1998) reported experiments that supported the sensory conflict theory rather than postural instability, although in relation to motion sickness rather than simulator sickness in VR. Keshavarz et al. (2015) review a number of studies that relatevection to visually induced motion sickness and conclude thatvection is a necessary but not sufficient prerequisite for motion sickness. In the context of VR, Ng et al. (2020) provided direct evidence in support of sensory conflict theory by that showing simulator sickness is minimized (based on the SSQ) when visual and physical motions are synchronously aligned.

In addition to questionnaire approaches such as the SSQ, attempts have been made to assess simulator sickness with physiological markers. The groundwork was laid by Kennedy et al. (2003) who showed that physiological responses could be used to classify different levels of severity of sickness in a flight simulator. Bertin et al. (2005), in the context of a driving simulator, investigated the relationship between simulator sickness as assessed by a subjective 'sickness score' ranging from 0 ("all is fine") to 10 ("I'm about to vomit") represented on a linear scale that participants could continually adjust. The physiological responses recorded were skin potential, skin resistance, skin temperature and heart rate.

There were effects shown in all 4 physiological responses between those who became sick and those who did not, most pronounced in skin resistance and temperature both of which were lower in the sick participants, with physiological results correlating with the sickness score. Li et al. (2022) measured skin temperature, ECG, vestibular function measurement (VNG), and skin colour on both cheeks, while motion sickness was induced in subjects on a rotating chair. A machine learning classifier was used to develop an objective assessment model for motion sickness based on combinations of these measures.

Another approach is to measure postural instability before and after exposure to the VR. For example, Sinitski et al. (2018) had participants walking on a treadmill in VR for 45 minutes and measured postural instability before and after the exposure, and found that although postural instability increased this was associated with mild simulator sickness symptoms that did not prevent participants from completing the task. With long VR exposures (up to 3 hours) Murata (2004) found postural instability to increase with time, arguing that the immersion experience was responsible both for simulator sickness and postural instability (so that it could not be inferred that postural instability was itself the cause of the simulator sickness). However, Arcioni et al. (2019) found that participants in VR with a predisposition to postural instability were more likely to experience simulator sickness irrespective of sensory conflict, and thus could be used as a method of prediction of disposition. In a VR study where participants were rotated by 15 degrees out of their body, and an expectation of simulator sickness, in fact little was found both with SSQ nor with extensive postural stability measures (Blom et al., 2014).

If sensory conflict is a primary cause or at least prerequisite for simulator sickness then diminishing the possibility of conflict provides an obvious way to reduce it. Fernandes and Feiner (2016) attempted this by dynamically reducing the visual field-of-view as a function of potential mismatch between physical and virtual motion. Hence while a participant was stationary the full field-of-view would be displayed, but diminished as they moved. They found that this method did reduce simulator sickness overall compared to no change in the field-of-view. A similar technique is to blur non-salient parts of the image, such as the periphery, during movement (Nie et al., 2019; Lin et al., 2020; Hussain et al., 2021). This technique also reduced simulator sickness compared to the control groups.

The virtual environment reported in (Barberia et al., 2018) alternated between simulated day and night. Participants were required to move through the environment by pressing a controller button (thus causing a strong mismatch between visual optical flow and vestibular sensations). In order to avoid serious simulator sickness, we had to make the maximum velocity of movement very slow. However, anecdotally we noticed that during the 'night' and hence darker phases of the experience, participants tended to move faster. Hence, we wondered whether speed of movement might be used as a surrogate for simulator sickness and whether symptoms could be modulated as a function of ambient light in the environment.

Our hypothesis was that darker environments would lead to greater speed, and that speed would be inversely proportional to the scores on the SSQ. In order to address this, we carried out two experimental studies. The results of the first led to a statistical model of how the velocity of moving through the environment was influenced by brightness. We found

that the SSQ was negatively correlated with speed, but that the darkness of the first exposure only, led to greater speed of movement through the environment and less simulator sickness. We then carried out a second study in order to test the statistical model derived from the first and found the model supported by these data. Our conclusion was that although all participants eventually adapt and increase velocity, at least in the specific conditions of this experiment, the level of brightness in the first exposure is critical.

Methods

Ethics

The experiment was approved by the Comissió de Biotètica, Universitat de Barcelona. Participants gave written and informed consent and all procedures were followed accordingly.

Materials

Both experiments were carried out using a Meta Quest 2. This has display resolution of 1832×1920 per eye with a field of view of 104 degrees horizontal, 98 degrees vertical and 113 degrees diagonal. The refresh rate is 90 Hz and the weight is 503 grams. It has 6 degrees of freedom head tracking. Participants held a controller in each hand but only the trigger on either hand was used for locomotion speed and the B button to stop early.

Scenario

The scenario consisted of a street of length 1256.5m with buildings at the side, and occasionally a bridge with buildings in the distance. In **experiment 1** the street consisted of 4 segments that alternated between brighter and darker ambient lighting. Participants were standing and were asked to move in a straight line along the whole length of the street by depressing the trigger button. The trigger button was connected to velocity by a simple curvilinear function such that initial pressing of the button would increase the velocity slightly but continual press of the button would increase the speed more. They would be stationary if the trigger button were not depressed, and could reach a maximum velocity of 12 metres per second if it were fully depressed. In **experiment 2** the street was the same except it was either bright throughout, or started off dark and gradually reached full brightness as the full length of the road was traversed. This was implemented using a day-night cycle which updated the lighting conditions according to the travelled distance, in a way that at the beginning was full darkness (night) and at the end of the path, full brightness (day). A real time directional light was used in this case and two main factors were updated according the travelled distance: the light's direction and colour. If we consider 't' as the normalized travelled distance, we have that for $t = 0$ (night, full darkness) the light's direction was (50, -30, 0) expressed in Euler angles, whilst light's colour was (1,1,1) in the normalized RGB format. On the other hand, at $t = 1$ (day, full brightness) the light's direction was (194, 0, 0) and colour was (0.1882, 0.1098, 0.0627). A linear distribution was used to update the lighting (direction and colour) thorough the path. Examples are shown in Figure 1 and Supplementary Video S1.

Experimental Design

Both experiments were between groups. In **experiment 1** there were two conditions: *Light First* where the first segment of the road was bright, and *Dark First* where the first segment of the road was dark. The brightness of the successive segments alternated between light and dark. There were two conditions in **experiment 2**: *Light* where the street was bright throughout, and *Dark* where the street started out dark but gradually increased in brightness as described above.

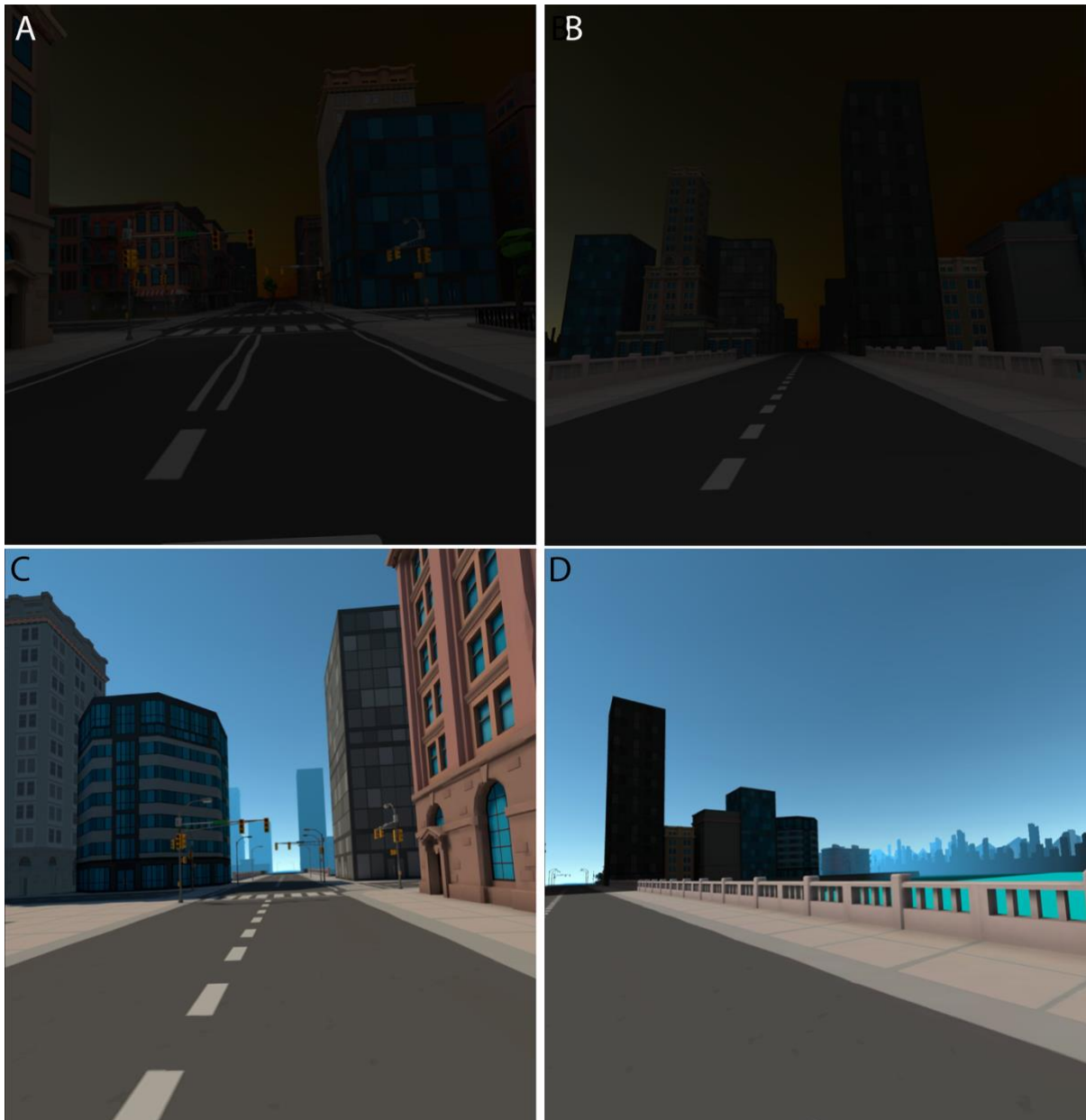


Figure 1 – The street used for the experiment. (A, B) different points along the dark street. (C,D) different points along the bright street.

Participants

Advertisements around the University campus requested interested participants to register on our laboratory data base that was available on Qualtrics (<https://www.qualtrics.com>). Participants had to be at least 18 years of age, and exclusion criteria included consumption

of alcohol at any time during the day of the experiment, taking any kind of psychoactive medication or any pathology that causes dizziness, being strongly susceptible to motion sickness in daily activities such as travelling in a vehicle, and having epilepsy. Participants also had to sign that they would not be driving a motor vehicle within 3 hours of completing the study.

There were 34 participants in **experiment 1**, 17 were randomly allocated to the *Light First* condition and 17 to the *Dark First*. The mean \pm SD age was 25.9 ± 8.47 , and 10 self-declared as male, 23 as female and 1 as other. Full details of the participant characteristics are available in Supplementary Table S1.

There were 36 participants in **experiment 2**, 18 were allocated randomly to the *Light* condition and 18 to the *Dark*. The mean \pm SD age was 23.5 ± 5.07 , 12 self-declared as male and the rest as female. Full details are available in Supplementary Table S1.

Implementation

The experiment was developed using Unity as the graphics engine. We also made use also of QuickVR (Oliva et al., 2022), a VR library for Unity which extends its VR capabilities and adds additional features such as avatar tracking, logic workflow management and locomotion systems.

The hardest part of the implementation was to optimize the scene for VR. We used as a base the city scene provided in this Unity package. Since we required the experiment to run on a wide variety of VR devices, from mobile (Quest, Pico) to desktop (HTC VIVE, Oculus Rift), we needed to spend some time on improving the overall framerate performance. We applied several optimization techniques in order to do so:

1. Polygon reduction: One of the most immediate optimization techniques consists of simplifying the geometry by reducing the number of polygons. For the simplest buildings, we just approximated them by using the closest 3D geometric primitive (cube, cylinder, hexagon...). Then we projected the original building onto the faces of the n-gon to generate the texture. For the most complex and intricate details, we used Simplygon, which is the standard for simplification on 3D gaming applications.
2. Texture optimization: We reduced the maximum resolution of textures to 2048×2048, but we also grouped several textures into a single one, producing what is known as an Atlas. This way, we could dramatically reduce the number of draw calls that the GPU needed to do since many objects can share the same material.
3. Object culling: As the participant follows a predefined path, we simply removed all the elements that were not visible from the point of view of the participant. Furthermore, the scene consisted of 4 identical patches, but they were not loaded all at once. Instead, they were loaded as the participant progressed through the path, and patches that were left behind a certain distance were progressively unloaded. Furthermore, each patch was subdivided into different chunks of buildings, so each chunk is loaded when the participant is at a specific distance, and unloaded when it is left behind.

4. Batch rendering: Unity allows for batch rendering, which means that the objects using the same material are grouped all together, so they can be rendered during the same GPU draw call.
5. Shadow optimization: We have been tweaking the shadow attributes in order to get the best compromise between render quality and performance.

This is an iterative process, so we were constantly checking the performance on the different target device, especially the low-end devices, to check the impact on performance of each step until we got a decent and stable framerate thorough the experience in all the devices.

Procedures

Upon arrival at the VR Lab, participants were asked to read an information sheet and consent form. After obtaining the signed consent, we told participants that they would be standing on a virtual street when they entered the VR. Then, we showed participants the controllers and described all the buttons and their functioning. We explained to participants that their task would be to move forward in the virtual street by using either of the trigger buttons on the left hand or right hand controllers, and the application would stop when they arrived at the end of the street. We also explained that forward velocity was positively correlated with how much the trigger was depressed.

We explained about simulator sickness and told participants to move as fast as possible along the road but slow enough not to experience simulator sickness. We explained that if they experienced simulator sickness or moved too fast, they should slow down by adjusting their speed with the trigger button. Participants were told that they were free to stop the experiment at any time without giving reasons, and could do so by pressing the B button on the right hand controller and informing the experimenter.

After the study description and information had been described, participants answered a questionnaire on the Qualtrics platform. This included the same information we previously had verbally explained in writing, and included a pre-questionnaire to be answered prior to the VR experience, and a post-questionnaire afterwards. The pre-questionnaire consisted of demographic questions about gender and age, questions regarding previous VR experience, knowledge of computer programming, video game playing frequency, as well as their proneness to motion sickness. After completing this pre-questionnaire, participants donned the head-mounted display and carried out the task.

When participants completed the virtual reality task, which took approximately 15 minutes, they removed the HMD, and continued with the post-questionnaire. This included the Simulator Sickness Questionnaire (SSQ) and some questions about their reactions to the light and dark parts of the street. The whole experimental session, including the ethics protocols, pre- and post-questionnaires, as well VR-exposure, lasted a maximum of 30 minutes. All the participants were compensated for their participation in the study with €10. Finally we debriefed participants about the purpose of the experiment.

Information about the time and velocity of movement of each participant was automatically recorded on a server. The questionnaire responses and information from the server were

tied together through a unique number that was generated at the end of the VR session and which participants had to write into the post-questionnaire.

Response Variables

There were two main response variables – the responses to the SSQ and velocity of movement along the road. The SSQ is further subdivided into the original components: scores for Nausea (nausea_ssq), Oculomotor Disturbance (oculomotor_ssq), Disorientation (disorientation_ssq) and the total score (ssq).

Statistical Methods

The analyses of the results of both experiments are in two parts. First, a descriptive analysis without formal statistical inference, and second, a statistical model. We use the Bayesian method to make inferences about the parameters of the model. This involves choosing prior distributions for each parameter which are updated by the data to produce posterior distributions. We can compute any probabilities of interest from the posterior distributions. The model includes all response variables simultaneously, so there is no issue with multiple comparisons (which results in problems in the interpretation of significance levels in classical null hypothesis testing). The model was evaluated using the Stan (mc-stan.org) probabilistic programming language (Carpenter et al., 2016) with RStudio (www.rstudio.com) using the rstan interface (mc-stan.org/users/interfaces/rstan). This was with 4 chains and 10000 iterations. The model converged without problem. See Supplementary Data S1 for the complete data and Stan program.

Results

Experiment 1

SSQ and velocity

Figure 2 shows the relationship between the total SSQ and overall mean velocity by condition. For those who started out in the light street there is a negative linear relationship. For those who started in the dark street the overall velocity is greater with one apparent outlier, and there is no relationship with SSQ.

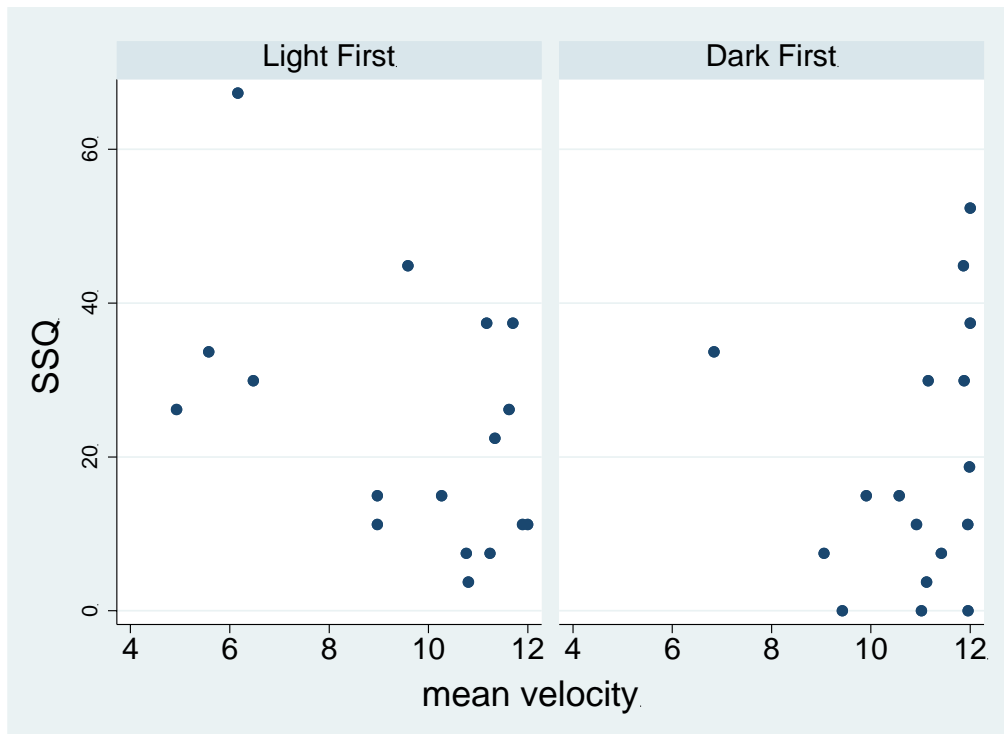


Figure 2 – Scatter diagram showing the relationship between total SSQ and mean velocity by condition.

Table 1 shows the correlations for each of the SSQ scores, indicating that there is no relationship between velocity and the nausea sub score, but there is a negative correlation with oculomotor and disorientation, but only in the condition where the first street segment was light. (The P values are only to give an idea about the strength of the correlation and are not meant for significance testing).

Table 1 – Pearson Correlations (r) between mean velocity and the SSQ scores, and their significance values (P)

SSQ	Light	Dark
nausea_ss q (r)	-0.15	0.28
P	0.565	0.280
oculomotor_ss q (r)	-0.49	0.19
P	0.048	0.476
disorientation_ss q (r)	-0.49	-0.14
P	0.047	0.600
ssq_total (r)	-0.45	0.14
P	0.067	0.601

Table 2 shows the mean SSQ scores by condition. The mean score is lower for each measure in the *Dark First* condition, and the effect size as measured by Cohen’s d is moderate for disorientation, and between small and moderate for the total.

Table 2 – Mean \pm Standard Error of the SSQ scores by condition (Light First, Dark First)

condition	nausea	oculomotor	disorientation	total
Light First	14.03 \pm 3.07	17.84 \pm 3.37	36.03 \pm 6.43	23.98 \pm 4.03
Dark First	12.91 \pm 4.48	16.05 \pm 3.11	21.29 \pm 6.22	18.70 \pm 3.98
Cohen's d	0.07	0.13	0.57	0.32

Velocity

It is not the case that participants move at greater overall velocity when the environment is dark. The bright street was experienced by those in the *Light First* condition in street segments 1 and 3, and by those in the *Dark First* condition in segments 2 and 4. Similarly the dark street was experienced by those in the *Light First* condition in segments 2 and 4 and for those in the *Dark First* condition in street segments 1 and 3. The mean velocity over all the bright streets was 10.3 ± 2.15 (SD), and over all the dark streets 10.18 ± 2.05 (SD). However, the brightness of the first street had an influence on velocity. Figure 3A shows the mean velocity per street segment showing that this increased over time tapering off to a maximum. Figure 3B shows the mean velocity by street segment and condition. Those in the *Dark First* condition moved at greater mean velocity through each street segment than those in the *Light First* condition.

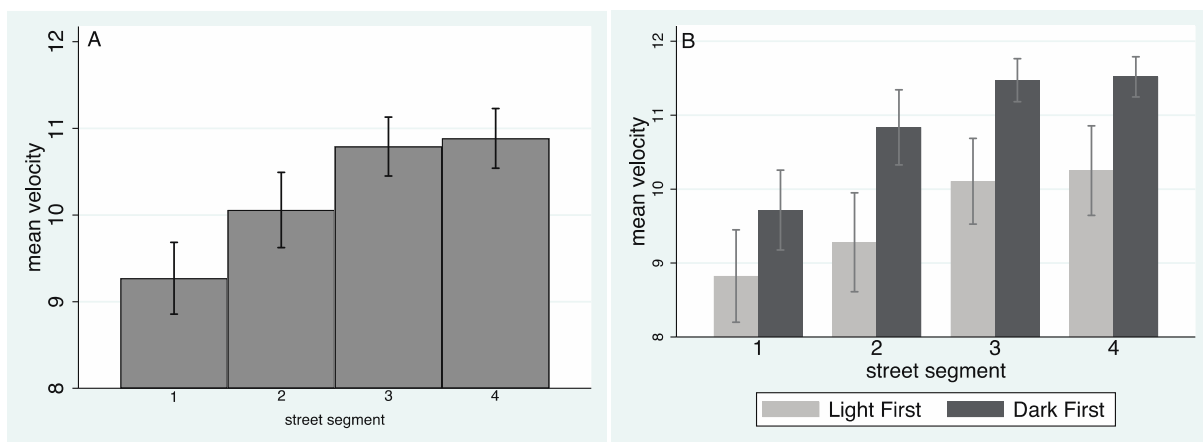


Figure 3 – Bar chart showing means and standard errors of velocity (A) By the first street encountered. (B) By the first street encountered and the condition.

Figure 4 shows the histograms of mean velocity by condition. Both histograms are clearly non-normally distributed, and the in the *Dark First* condition the density is greater towards the maximum velocity.

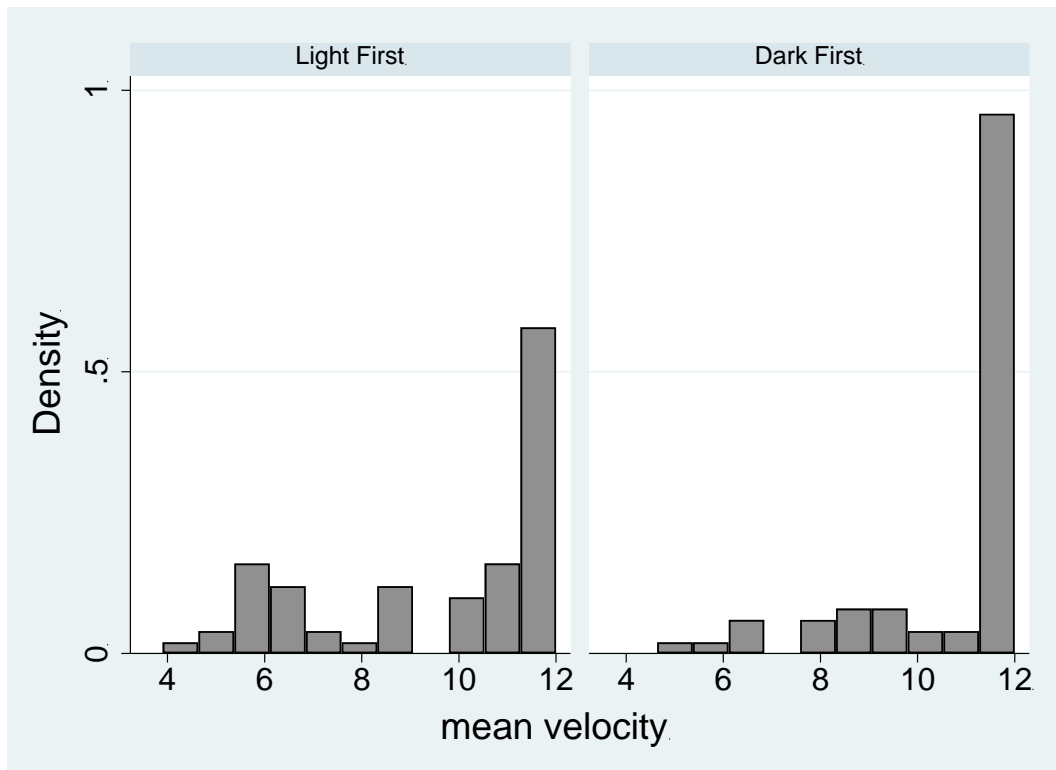


Figure 4 – Histogram of mean velocity by condition

Conclusion from descriptive analysis

The brightness of the first street influences velocity, with greater velocity if the first street is dark, and greater velocity is associated with lower simulator sickness. However, considering a street-by-street level, dark streets do not seem to lead to greater velocity than light streets. The confounding issue is that velocity is influenced by two factors: the order of the street (greater velocity for later streets tapering off to a maximum), and the brightness. We next consider a statistical model that accounts for these two factors.

Statistical model

As can be seen in Figure 3 both street segment and brightness contribute to velocity, in a non-linear way – i.e., velocity increases but levels out at a maximum. Here we present a model that attempts to separate out their influence.

Considering Figure 3A the relationship between velocity (V) and street number (S) is of the form:

$$V = \alpha - \gamma e^{-\theta \cdot S} \quad (1)$$

where $\alpha, \gamma > 0, \theta > 0$ are parameters with unknown value. As S increases V increases but up to the theoretical limit of α . However, the model should also allow darkness ($D = 0$ light, $D = 1$, dark) to modify the outcome.

Consider the model with linear predictor:

$$\eta_i = u_{id_i} + \beta_0 + \beta_1 D_i - \beta_2 \exp(-\beta_3 S_i (D_i \lambda + 1 - D_i)) \quad (2)$$

$$i = 1, 2, \dots, N = 136$$

When $D_i = 0$ (light) this reduces to the same form as (1). When $D_i = 1$ (dark) then through β_1 the velocity may be changed, and similarly the rate of decay would also depend on the parameter λ . The relationship is easier to see as:

$$\eta_i = \begin{cases} u_{id_i} + \beta_0 - \beta_2 \exp(-\beta_3 S_i), & \text{when } D_i = 0 \\ u_{id_i} + \beta_0 + \beta_1 - \beta_2 \exp(-\beta_3 S_i \lambda), & \text{when } D_i = 1 \end{cases}$$

u_{id_i} is a random effects term, since each participant traverses 4 streets, and therefore the model must allow for variations between participants – the 136 observations are not independent, but may be clustered by participant. id_i is the identifier for the participant in the i th trial. Hence id is of the form: 1,1,1,1, 2,2,2,2, ..., n, n, n, n (where $n=34$), with the ids labelled from 1 to n .

Instead of using the raw data for velocity we transform it to the interval $[0,1]$, and refer to the transformed variable as v . Instead of the assumption of a normal distribution, we use the Beta distribution as a model for this linearly transformed response variable, conditional on the parameters since Figure 4 indicates great departure from normality. The Beta distribution was chosen since it can adapt to many different shapes (skewed, J-shaped, reverse-J, U shaped, symmetrical around 0.5 with the mode at 0.5, etc.) depending on the parameters, and it is bound to the $[0,1]$ range.

The Beta distribution has two parameters, $\alpha > 0$ and $\beta > 0$, referred to as the $Beta(\alpha, \beta)$ distribution, which has mean $\frac{\alpha}{\alpha + \beta}$. The probability density is 0 outside of the range $[0,1]$.

For the response variable v the likelihood function (the probability distribution of the data conditional on the parameters) is

$$v_i \sim Beta(\phi \mu_i, \phi(1 - \mu_i)), 0 < v_i < 1 \quad (3)$$

which ensures that the mean is μ_i . The parameter $\phi > 0$ is a scale parameter and is not of any interest here.

We want to relate the mean μ_i to the linear predictor (2), but since $\mu_i \in [0,1]$ the standard approach is to use the logit link function (the link function relates the mean to the linear predictor), in this case the log odds:

$$\log\left(\frac{\mu_i}{1 - \mu_i}\right) = \eta_i \quad (4)$$

Therefore, the inverse link function is:

$$\mu_i = \frac{1}{1 + e^{-\eta_i}} \quad (5)$$

Hence the overall model is given by (2), (3) and (5).

The prior distributions chosen:

$$\begin{aligned} \beta_j &\sim \text{normal}(\text{mean} = 0, \text{SD} = 2), \\ \phi &\sim \text{Gamma}(\text{shape} = 2, \text{rate} = 0.1), \phi > 0 \\ u_{id_i} &\sim \text{normal}(\text{mean} = 0, \text{SD} = 2) \\ \lambda &\sim \text{Gamma}(\text{shape} = 2, \text{rate} = 0.1), \lambda > 0 \end{aligned}$$

Posterior distributions

Table 3 shows the summaries of the posterior distributions of the parameters. β_1 is one way that darkness might directly influence velocity. However, the 95% credible interval for this parameter well includes 0 and the probability of the parameter being positive is 0.669. The evidence is not strong enough to infer that $\beta_1 > 0$. The second way that darkness can influence velocity in this model is through the parameter λ . The greater the value of λ the higher the velocity for each street segment if $\beta_2 > 0$, which is almost certain. For increasing values of $\lambda > 1$, $\beta_2 \exp(-\beta_3 S_i \lambda) < \beta_2 \exp(-\beta_3 S_i)$ indicating that the velocity for the *Dark First* condition will be greater than the *Light First*. The mean of the distribution of λ is 2.64, and the median is 2.12. The probability of $\lambda > 1$ is 0.88. This is illustrated in Figure 5 which shows the probabilities $P(\lambda > x)$ for increasing values of x .

Table 3 - Summaries of the posterior distributions of the model showing the means, standard deviations and 95% credible intervals. Prob > 0 contains the posterior probabilities of the parameter being positive.

Parameter	Mean	SD	2.5%	97.5%	Prob > 0
β_0	2.79	0.77	1.39	4.41	1.000
β_1	0.38	0.91	-1.47	2.12	0.669
β_2	3.56	0.62	2.42	4.86	1.000
β_3	0.42	0.24	0.13	1.04	1.000
λ	2.64	1.93	0.61	7.39	
ϕ	4.95	0.77	3.58	6.58	

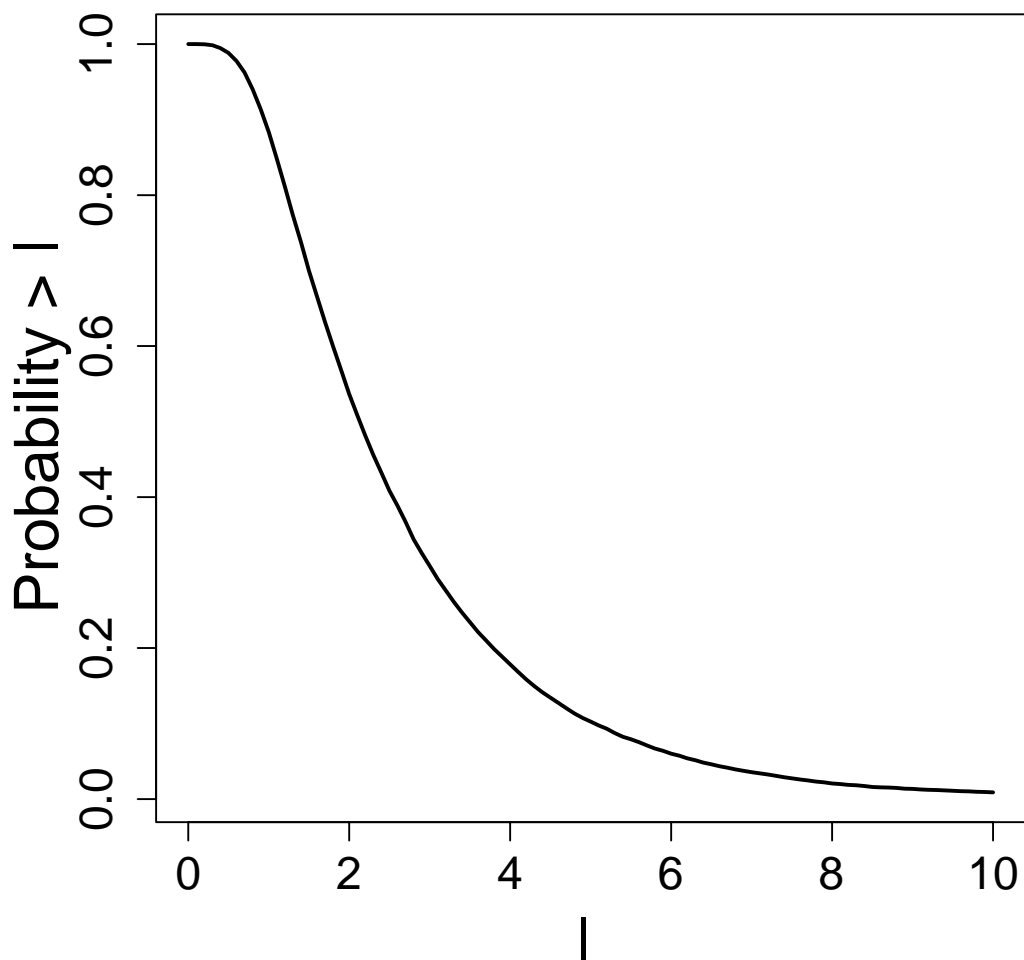


Figure 5 – The survivor function for λ : the probability of being $> \lambda$

Overall the model indicates that velocity is likely to be greater for the *Dark First* condition than the *Light First*. We discuss the overall goodness of fit of the model later.

Experiment 2

Recall that in experiment 2 there were again 2 conditions, Light where the street was light throughout, and Dark where the street started out dark and gradually became light over the course of the traversal. In order to use the statistical model above we nevertheless partition the street into 4 equal segments for analysis, exactly as for experiment 1. There were 18 participants in each condition, with mean \pm SD age 23.5 ± 5.07 , and 12 identified as male and the rest as female. Full details are available in Supplementary Table S2.

SSQ and velocity

Figure 6 demonstrates a very similar relationship between SSQ and mean velocity as experiment 1 (Figure 2). There is a negative association in the Light condition and no association in the Dark condition, since generally the velocities are higher except for two outliers. Table 4 shows the correlations with the components of the SSQ, and in this case all components are negatively correlated in the Light condition, and none in the Dark condition.

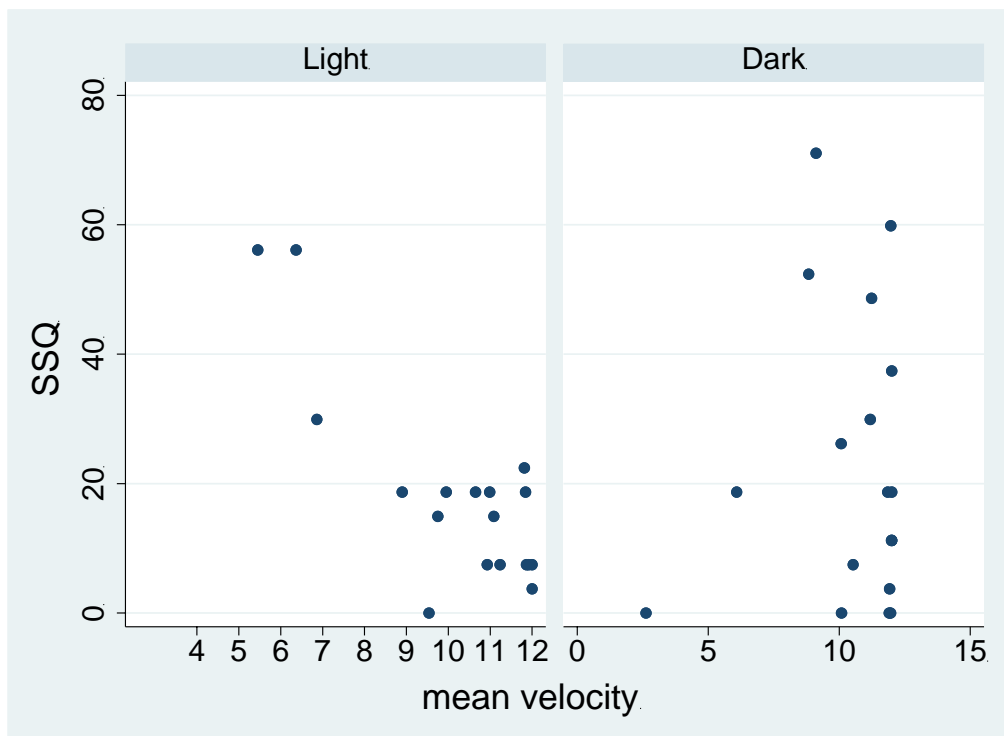


Figure 6 – Scatter diagram showing the relationship between total SSQ and mean velocity by condition (experiment 2)

Table 4 – Pearson Correlations (r) between mean velocity and the SSQ scores, and their significance values (P)

SSQ	Light	Dark
nausea_ssq (r)	-0.50	0.01
P	0.037	0.955
oculomotor_ssq (r)	-0.80	0.01
P	0.000	0.977
disorientation_ssq (r)	-0.61	0.11
P	0.007	0.667
ssq_total (r)	-0.819	0.053
P	0.000	0.8339

Table 5 shows the mean SSQ scores by condition. The mean score is lower in the Dark condition for each measure, but the effect size is moderate only for disorientation. As was the case for experiment 1 the greatest difference is for disorientation.

Table 5 – Mean \pm Standard Error of the SSQ scores by condition (Light, Dark) - experiment 2

condition	nausea	oculomotor	disorientation	total
Light	13.25 \pm 4.30	18.11 \pm 4.47	33.25 \pm 8.20	23.06 \pm 5.27
Dark	12.72 \pm 3.93	14.74 \pm 3.70	22.43 \pm 4.79	18.28 \pm 3.69
Cohen's d	0.03	0.19	0.38	0.25

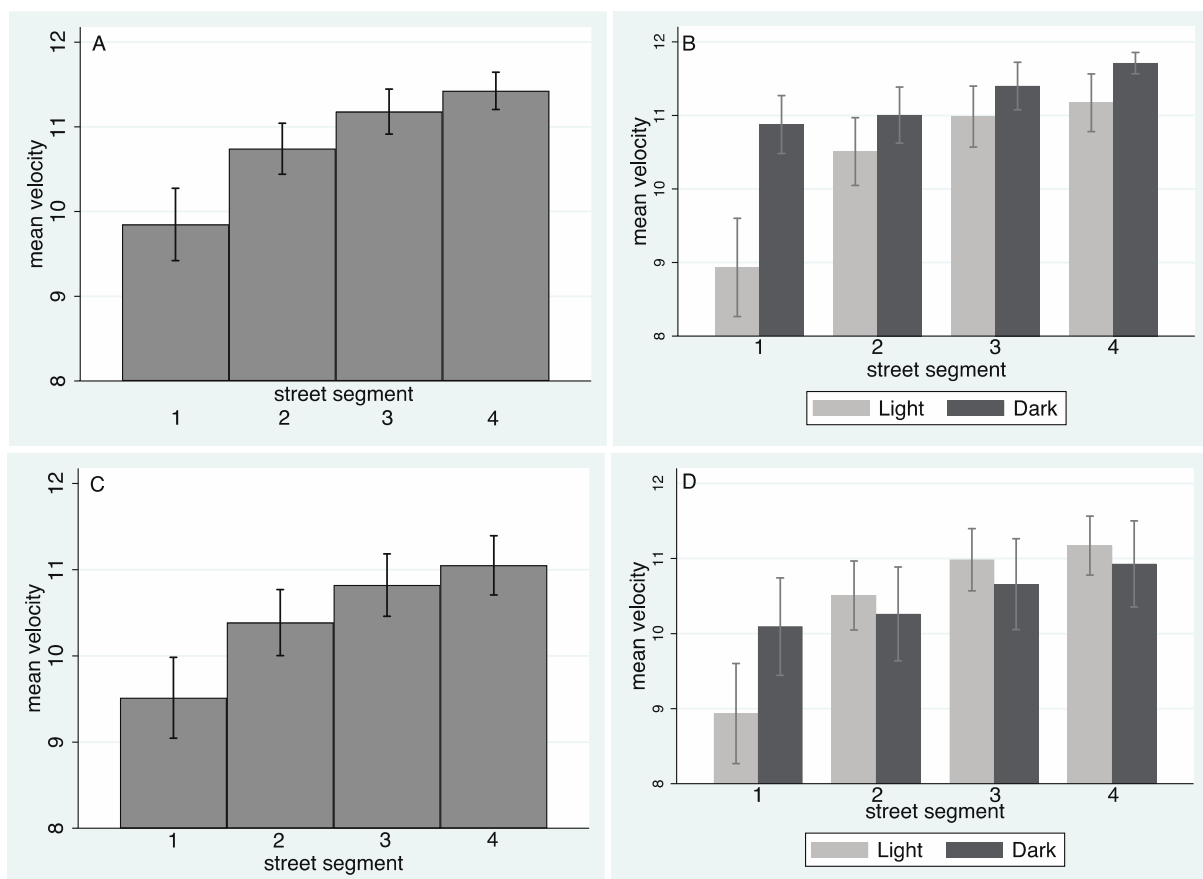


Figure 7 – Bar chart showing means and standard errors of velocity for experiment 2 (A) By the street encountered without the outliers shown in Figure 6 (Dark). (B) By street and condition without the outliers shown in Figure 6 (Dark). (C) By street encountered using all data (D) By street encountered and condition using all data.

Velocity, SSQ and Brightness

Figure 7A shows the means and standard errors of velocity by street, and Figure 7B also by condition, but without the two outliers shown in Figure 6 (Dark). Figure 7C and Figure 7D show the same but including those outliers. These again follow the same pattern

as experiment 1 (Figure 3). Notice that in the first street the velocity in the Dark condition is clearly greater than the Light condition, but then over time the two velocities become almost the same when the outliers are included but are almost the same as experiment 1 (Figure 3B) when the outliers are excluded. For both conditions the velocities increase and taper off.

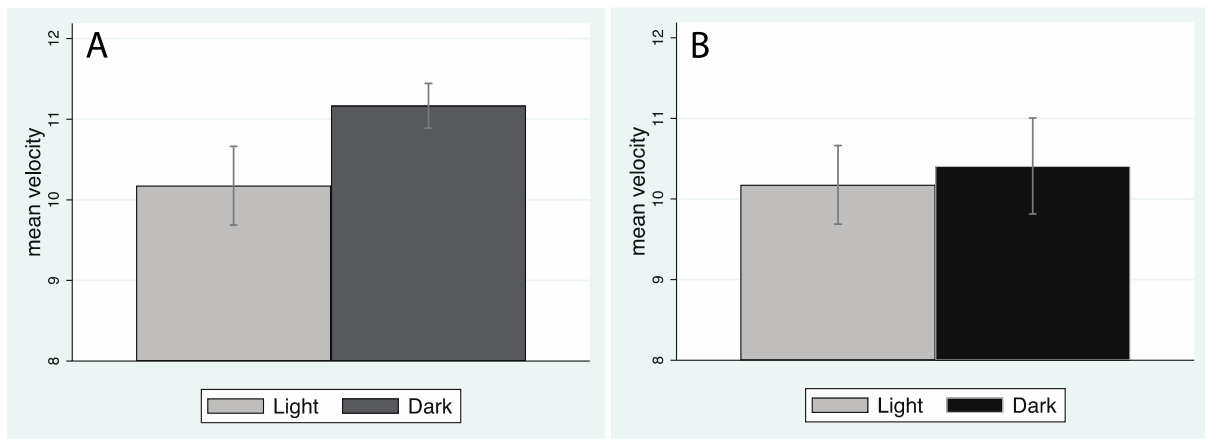


Figure 8 – Bar charts showing the means and standard errors of velocity by condition. (A) With the outliers from Figure 6 (Dark) excluded. (B) For all data.

Figure 8 shows the bar charts of means and standard errors of velocity by condition. Figure 8A excludes the outliers found in Figure 6. Cohen's d for the difference of the two means is 0.59 which is above what is normally regarded as 'moderate'. Figure 6B shows that when all the data is used, including the two outliers, then the means are almost the same (Cohen's $d = 0.10$).

Conclusion from descriptive analysis

Over time both groups adapt (Figure 7). However, the group that starts in the dark environment has an initial advantage with respect to velocity. Since the velocity is already high, there is not great room for improvement – i.e., there is a ceiling effect that applies earlier than for the Light group. The results are very similar to experiment 1, especially when the outliers are excluded. Moreover, now we can use the predictive statistical model from experiment 1 and test this with experiment 2.

Posterior distributions

Table 6 shows the summaries of the posterior distributions of the parameters based on all the data. We do not exclude the outliers in order not to potentially bias the results in favour of the hypothesis that we started with. The results are qualitatively similar to experiment 1. In particular there is a low probability that $\beta_1 < 0$ (probability = $1 - 0.24 = 0.76$). $\beta_2 > 0$ and $\beta_3 > 0$ with probability 1, and $\lambda > 1$ with probability 0.988. Figure 9 shows the probabilities $P(\lambda > x)$ for increasing values of x . Even for $\lambda = 4$ the probability is still greater than 0.8.

Table 6 - Summaries of the posterior distributions of the model showing the means, standard deviations and 95% credible intervals for experiment 2. Prob > 0 contains the posterior probabilities of the parameter being positive

Parameter	Mean	SD	2.5%	97.5%	Prob > 0
β_0	2.97	0.57	1.89	4.12	1.00
β_1	-0.49	0.72	-1.89	0.94	0.24
β_2	3.81	0.90	2.19	5.75	1.00
β_3	0.75	0.27	0.30	1.34	1.00
λ	16.54	14.00	1.67	52.35	
ϕ	5.68	0.93	4.03	7.68	

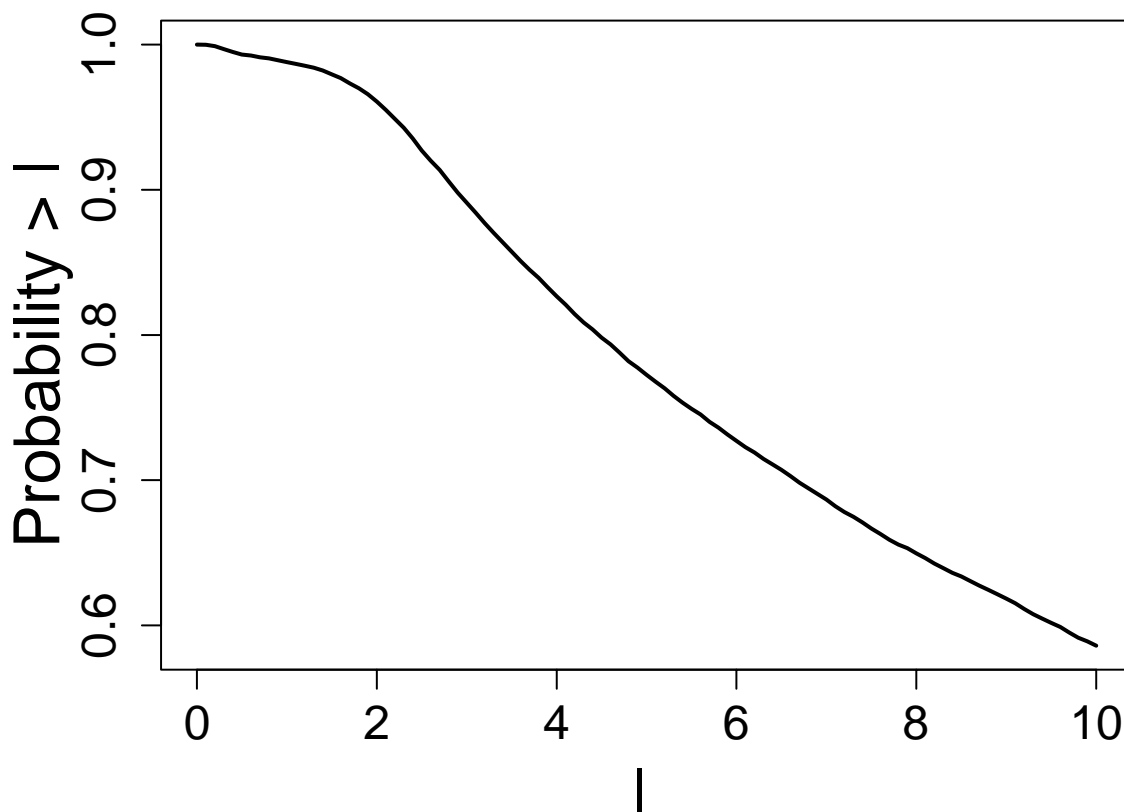


Figure 9– The survivor function for λ : the probability of being > λ

Predictions and goodness of fit for both experiments

We can derive posterior distributions of velocity based on the posterior distributions of the model parameters for each condition, and each level of street. Figure 10 shows these distributions for each street segment, comparing the Light and Dark conditions. In each case there is a large difference between the Light (First) and Dark (First) conditions in both

experiments for street 1, which is maintained throughout in experiment 1, but for experiment 2 the difference is minimal by street 3.

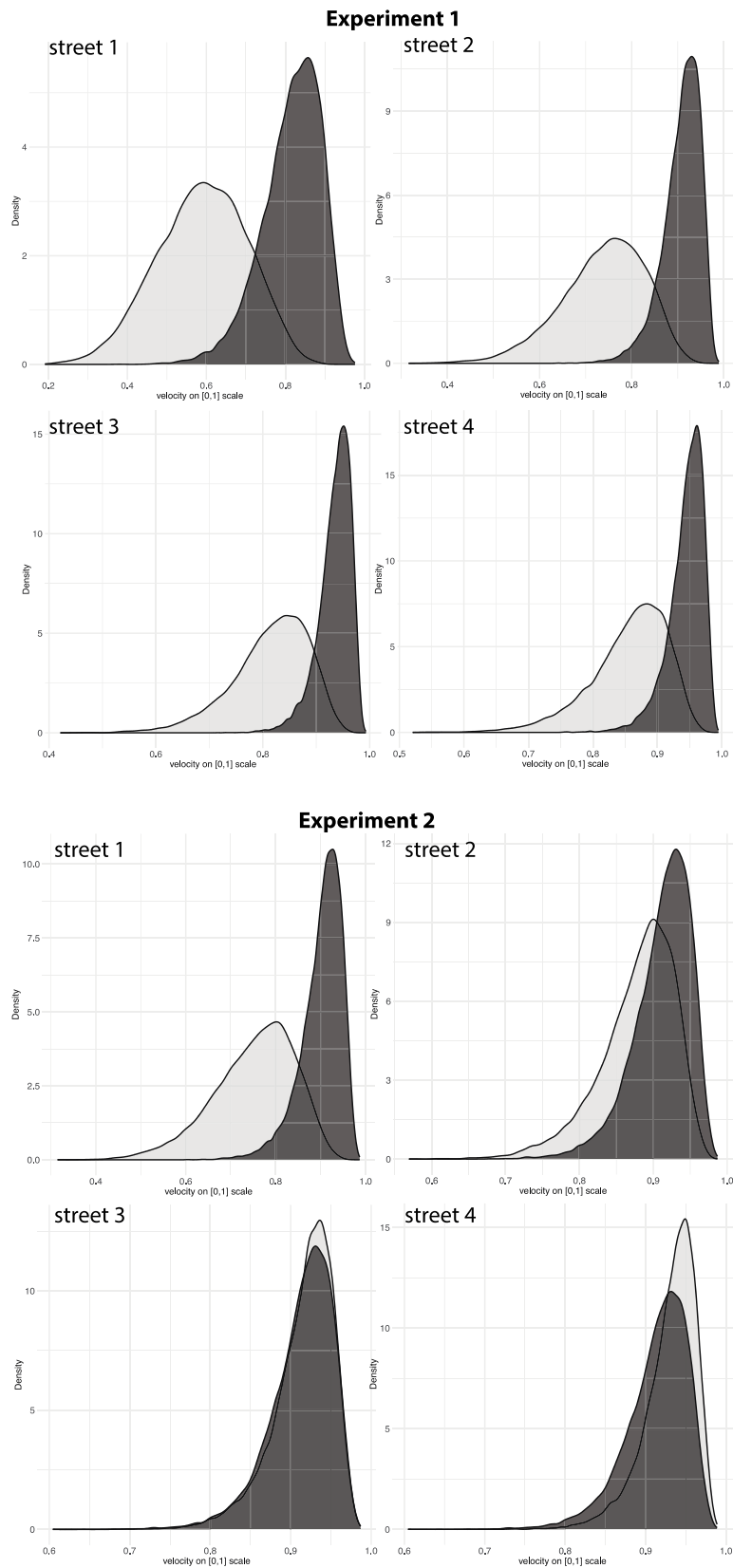


Figure 10 – probability density functions for the posterior distributions of velocity for each street by condition (light, dark) for both experiments

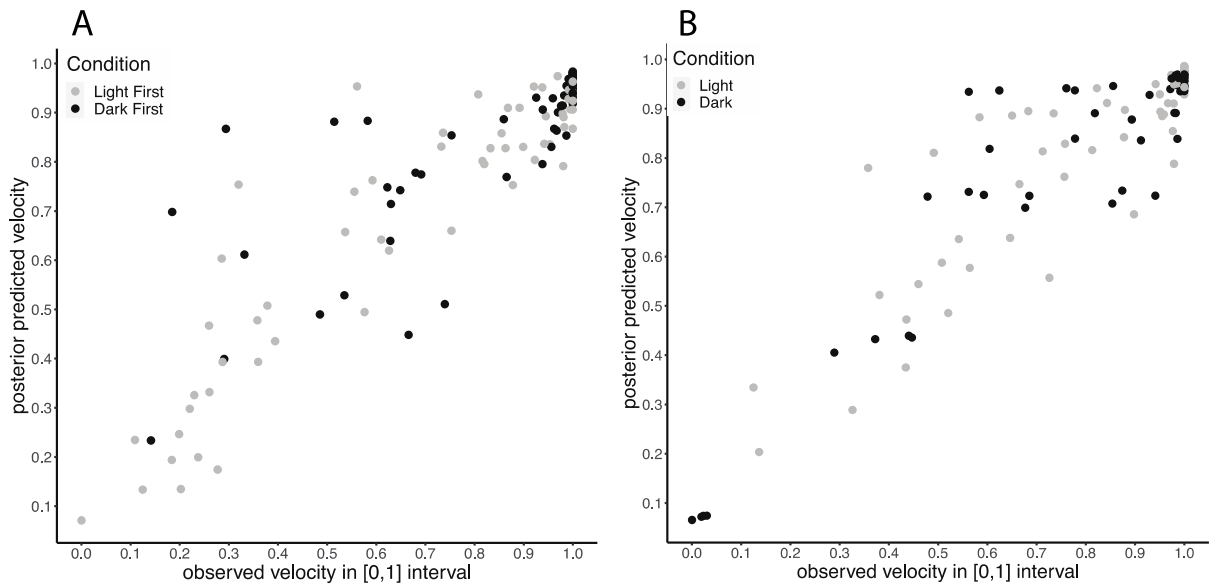


Figure 11 – Means of the posterior predicted distributions of velocity by observed velocity (A) experiment 1 (B) experiment 2.

In order to examine how well the model fits the data, new simulated observations on velocity can be generated from the model, and compared with the observed values (transformed to the [0,1] interval). For each individual record a posterior probability distribution of the velocity is generated. These are called the ‘predicted posterior distributions’. The mean of each distribution is a point estimate of the predicted velocity for that record. Figure 11 shows the scatter plots of the means of the predicted posterior distributions of velocity against the true values. The fits are very good. For experiment 1 the correlation between the predicted and observed values is $r = 0.901$, $P < 2.2 \times 10^{-16}$, and for experiment 2, $r = 0.92$, $P < 2.2 \times 10^{-16}$.

As a further test of the appropriateness of the model we used the ‘leave one out’ cross-validation (loo) method (Vehtari and Gelman, 2014). Here a single observation is left out of the dataset, and the model is estimated using the remaining data, which is then used to compute the prediction error for the left-out observation. This process is repeated for all observations in the dataset, and the results are used to estimate the model’s out-of-sample predictive performance. So-called ‘Pareto k estimates’ derived from this analysis provide a diagnostic measure used to assess the validity of model. The Pareto k statistic identifies observations that may have a significant impact on the model’s predictive performance – i.e., it identifies potential outliers. The Pareto k statistic is calculated for each observation. A high Pareto k value (greater than 0.7) indicates that the observation may have an undue influence on the model. In experiment 1 there was one outlying value with Pareto $k > 0.7$ and in experiment 2, Pareto $k < 0.7$ for all observations.

Discussion

Our initial hypothesis was that participants would tend to traverse faster through a virtual environment which has a low level of ambient light than a brighter environment. This was not supported in experiment 1, where participants alternated between a dark and brighter street, since the overall mean velocity was almost the same over all the dark streets as the light streets. However, the illumination of the first street encountered did have an impact, with those who started in the dark street travelling at greater mean velocity compared with those who started out in the light street first (Figure 3B). In experiment 2 all but two of the participants moved with greater mean velocity in the street that started out dark and gradually became light, compared with those who were on the street that was always light (Figure 7B).

The second objective was to examine the relationship between velocity and simulator sickness, with the idea that these would be negatively correlated in our setup. Here both experiments had similar findings. In experiment 1 there was a negative correlation between velocity and the SSQ for those in the Light First condition and no correlation for those in the Dark First condition (Figure 2) where the mean velocities were uniformly greater. Oculomotor and disorientation sub-categories of the SSQ rather than nausea accounted for this (Table 1). In experiment 2 the same relationship was found, a negative correlation for the Light Condition and no correlation for the Dark condition (Figure 6). This was also the case for all three components of the SSQ (Table 4). It is well known that there is usually a positive correlation between velocity and simulator sickness in experimental studies (Chardonnet et al., 2015). Widdowson et al. (2021) measured SSQ for three different modes of displacement through a virtual hallway – constant velocity, a ramp where the velocity increased and then decreased linearly, and polynomial increase and decrease. The SSQ increased compared to a baseline in each case, but there was no evidence that the constant velocity was more effective in reducing sickness compared with the others. In these experimental studies participants do not have control over the velocity, since they are subject to different velocities as part of the experimental design. In our study participants were told to only go as fast as comfort allowed and were able to adjust their speed accordingly. This resulted in the negative correlation of velocity and SSQ, but only in the Light First or Light conditions. Giving participants the instruction to adjust their speed according to their level of sickness makes velocity an objective surrogate for sickness, other things being equal.

The third major objective was to construct a statistical model for the results of experiment 1, and then use the same form of model for the analysis of the results of experiment 2. The models provided excellent fits to these data. The analysis confirmed the descriptive findings, that for experiment 1 the Dark First condition produced better overall outcomes for simulator sickness and in experiment 2 the Dark condition did so – in spite of including two clear outliers in the data used for the analysis. Both sets of results together strongly suggest that the first exposure is critical – if it is dark then the effect on simulator sickness carries over to the subsequent navigation through the environment.

The method we have introduced is most similar to Fernandes and Feiner (2016) who reduced simulator sickness by restricting the field of view while moving, and the techniques

to blur the periphery (Nie et al., 2019; Lin et al., 2020; Hussain et al., 2021). We argue that though these methods are similar in the sense of reducing sensory conflict the method exploiting darkness has two advantages. The first is that it is 'natural' in the sense that people do carry out activities in darkness, and restrictions of field of view or blurring may cause breaks-in-presence (Slater and Steed, 2000) although Fernandes and Feiner (2016) argued that presence is maintained when their technique is employed. Second, even though the environment is darker, participants can nevertheless perceive the whole structure of the environment (e.g., there is a building on the left, a river to the right, and so on) at all times. This is particularly important during navigation – since critical areas of the visual field being shut down during movement, may lead to disorientation in the sense that participants may not see important landmarks during their movement, and thus wayfinding would be adversely affected. For example, a larger field-of-view positively influences distance judgements (Masnadi et al., 2022).

The visual system operates differently in relative darkness compared to brighter environments, with varying activations of the photoreceptor rod and cone cells on the retina. Jonas et al. (1992) in a study of 21 human cornea donors found the mean number of rods to be 60,123,000 and cones 3,173,000 (with huge variances in both cases), though it is generally accepted that there are about 120 million rod cells and 6 million cone cells. See also the NIH report (Purves et al., 2001). The cone cells in daylight are those that are mainly active, responsible for visual acuity and colour vision, and are highly concentrated in a relatively tiny area of the retina called the fovea. During daylight the rods are responsible for peripheral vision, especially responding to movement in the periphery, and have much less acuity. The rods are highly sensitive to light and motion and become more active in night time conditions but are not sensitive to colour. Hence vision in the dark is mediated primarily by the system of rods since they have the much greater sensitivity to light, but colour perception, visual acuity and depth perception are low. Hence, in darker conditions there is less visual load, acuity, detail, which possibly mitigates the conflict between the vestibular and sensorimotor systems, thus reducing simulator sickness. Darker environments may therefore overcome the discrepancies that according to the sensory conflict theory are a major cause of simulator sickness. A further experimental study is needed to test this explanation. This would involve participants being exposed to a dark environment for at least 30 minutes to give adequate time for full adaptation, followed by a series of tasks that would normally cause simulator sickness. It would then be interesting if after such a period of adaptation and task performance whether low simulator sickness would be maintained in conditions of gradually increasing brightness. The question is whether the brain somehow learns during the dark period to operate in VR without simulator sickness, and then carries over that learning to a brighter environment.

There has been a huge amount of work on simulator sickness over the past 3 decades and also a substantial literature on motion sickness. With respect to simulator sickness in VR this is reflected in the number of review and meta studies, further highlighting its importance – for example (Davis et al., 2014; Leung and Hon, 2019; Chang et al., 2020; Saredakis et al., 2020; Caserman et al., 2021; de Winkel et al., 2022; Li et al., 2023). It is also important to take into account that while system factors such as rendering and tracking latency are obviously critical, and which have been the main focus of many studies, individual

differences are also important to achieve a full explanation and mitigation of sickness (Howard and Van Zandt, 2021). Individual differences may also be activated through different belief systems of individuals (Nooij et al., 2021) – it is likely that some readers will have encountered individuals who claim “I never get simulator sickness” and indeed they never report it.

There are two main limitations to our study that would need to be overcome in future work. The first is that the greatest velocity attainable (12 m per s) was nevertheless quite slow. This was deliberate, in order to minimise the level of discomfort for participants. Our prediction is that if greater velocities had been allowed then the difference between the dark and light conditions would have been more pronounced – i.e., the Dark First or Dark conditions would have been substantially different to the Light First or Light conditions. The second limitation is that we only considered translational velocity – participants moved in a straight line. They could look anywhere, but there was no rotation. Lo and So (2001) found significant increases in simulator sickness due to rotation, and we do not know whether darkness would alleviate this.

Overall our results suggest that allowing participants to control their translational velocity, and starting the VR exposure with a dark environment could provide a useful way to minimise simulator sickness, and experiment 2 suggests that the light can gradually be increased without adverse effects. However, further studies on the lines suggested above would be needed. In both experiments we found that over time participants were able to achieve approximately the same velocity levels irrespective of condition, and therefore it could be argued that the initial darkness period is not needed. In other words there is adaptation notwithstanding the earlier levels of darkness. However, the early part of an exposure to a VR scenario is crucial – since people may withdraw if they quickly encounter strong simulator sickness, and thereby decide to never try VR again. When people first enter any virtual environment we should strive to do everything possible to achieve comfort – ranging from the design and weight of head-mounted displays through to the minimisation of the possibility of simulator sickness.

Acknowledgments

This research was supported by the European Research Council Advanced Grant MoTIVE (#742989), and the GuestXR project which has received funding from the European Union’s Horizon 2020 research and innovation programme under grant agreement No. 101017884. ES is partially supported by a PhD studentship from Facebook. GS was supported by La Caixa Foundation (ID 100010434) with Fellowship code LCF/BQ/DR19/11740007.

References

- Arcioni, B., Palmisano, S., Apthorp, D., and Kim, J. (2019). Postural stability predicts the likelihood of cybersickness in active HMD-based virtual reality. *Displays* 58, 3-11.
- Balk, S.A., Bertola, D.B., and Inman, V.W. (Year). "Simulator sickness questionnaire: twenty years later", in: *Driving Assessment Conference*: University of Iowa).

- Barberia, I., Oliva, R., Bourdin, P., and Slater, M. (2018). Virtual mortality and near-death experience after a prolonged exposure in a shared virtual reality may lead to positive life-attitude changes. *PLoS one* 13, e0203358. doi.org/10.1371/journal.pone.0203358
- Bertin, R., Collet, C., Espié, S., and Graf, W. (Year). "Objective measurement of simulator sickness and the role of visual-vestibular conflict situations", in: *Driving Simulation Conference North America: University of Central Florida Orlando, USA*, 280-293.
- Bimberg, P., Weissker, T., and Kulik, A. (Year). "On the usage of the simulator sickness questionnaire for virtual reality research", in: *2020 IEEE conference on virtual reality and 3D user interfaces abstracts and workshops (VRW): IEEE*, 464-467.
- Blom, K.J., Arroyo-Palacios, J., and Slater, M. (2014). The effects of rotating the self out of the body in the full virtual body ownership illusion. *Perception* 43, 275-294. doi.org/10.1068/p76
- Carpenter, B., Gelman, A., Hoffman, M., Lee, D., Goodrich, B., Betancourt, M., Brubaker, M.A., Guo, J., Li, P., and Riddell, A. (2016). Stan: A probabilistic programming language. *Journal of Statistical Software* 20. doi.org/10.18637/jss.v076.i01
- Caserman, P., Garcia-Agundez, A., Gámez Zerban, A., and Göbel, S. (2021). Cybersickness in current-generation virtual reality head-mounted displays: systematic review and outlook. *Virtual Reality* 25, 1153-1170.
- Chang, E., Kim, H.T., and Yoo, B. (2020). Virtual reality sickness: a review of causes and measurements. *International Journal of Human-Computer Interaction* 36, 1658-1682.
- Chardonnet, J.-R., Mirzaei, M.A., and Mérienne, F. (Year). "Visually induced motion sickness estimation and prediction in virtual reality using frequency components analysis of postural sway signal", in: *International conference on artificial reality and telexistence eurographics symposium on virtual environments*, 9-16.
- Davis, S., Nesbitt, K., and Nalivaiko, E. (Year). "A systematic review of cybersickness", in: *Proceedings of the 2014 conference on interactive entertainment*, 1-9.
- De Winkel, K.N., Talsma, T.M., and Happee, R. (2022). A meta-analysis of simulator sickness as a function of simulator fidelity. *Experimental Brain Research*, 1-17.
- Fernandes, A.S., and Feiner, S.K. (Year). "Combating VR sickness through subtle dynamic field-of-view modification", in: *2016 IEEE Symposium on 3D User Interfaces (3DUI): IEEE*, 201-210.
- Howard, M.C., and Van Zandt, E.C. (2021). A meta-analysis of the virtual reality problem: Unequal effects of virtual reality sickness across individual differences. *Virtual Reality* 25, 1221-1246.
- Hussain, R., Chessa, M., and Solari, F. (2021). Mitigating cybersickness in virtual reality systems through foveated depth-of-field blur. *Sensors* 21, 4006.
- Jonas, J.B., Schneider, U., and Naumann, G.O. (1992). Count and density of human retinal photoreceptors. *Graefe's Archive for Clinical and Experimental Ophthalmology* 230, 505-510.
- Kennedy, R., Drexler, J., Compton, D., Stanney, K., Lanham, D., and Harm, D. (2003). Configural scoring of simulator sickness, cybersickness and space adaptation syndrome: similarities and differences. *Virtual and adaptive environments: Applications, implications, and human performance issues*, 247.
- Kennedy, R.S., Lane, N.E., Berbaum, K.S., and Lilienthal, M.G. (1993). Simulator sickness questionnaire: An enhanced method for quantifying simulator sickness. *The international journal of aviation psychology* 3, 203-220.

- Keshavarz, B., Riecke, B.E., Hettinger, L.J., and Campos, J.L. (2015). Vection and visually induced motion sickness: how are they related? *Frontiers in psychology* 6, 472.
- Kolasinski, E.M. (1995). Simulator sickness in virtual environments.
- Leung, A.K., and Hon, K.L. (2019). Motion sickness: an overview. *Drugs in context* 8.
- Li, C.-C., Zhang, Z.-R., Liu, Y.-H., Zhang, T., Zhang, X.-T., Wang, H., and Wang, X.-C. (2022). Multi-dimensional and objective assessment of motion sickness susceptibility based on machine learning. *Frontiers in Neurology* 13.
- Li, X., Luh, D.-B., Xu, R.-H., and An, Y. (2023). Considering the Consequences of Cybersickness in Immersive Virtual Reality Rehabilitation: A Systematic Review and Meta-Analysis. *Applied Sciences* 13, 5159.
- Lin, Y.-X., Venkatakrishnan, R., Venkatakrishnan, R., Ebrahimi, E., Lin, W.-C., and Babu, S.V. (2020). How the presence and size of static peripheral blur affects cybersickness in virtual reality. *ACM Transactions on Applied Perception (TAP)* 17, 1-18.
- Lo, W., and So, R.H. (2001). Cybersickness in the presence of scene rotational movements along different axes. *Applied ergonomics* 32, 1-14.
- Masnadi, S., Pfeil, K., Sera-Josef, J.-V.T., and Laviola, J. (Year). "Effects of field of view on egocentric distance perception in virtual reality", in: *Proceedings of the 2022 CHI Conference on Human Factors in Computing Systems*, 1-10.
- Murata, A. (2004). Effects of duration of immersion in a virtual reality environment on postural stability. *International Journal of Human-Computer Interaction* 17, 463-477.
- Ng, A.K., Chan, L.K., and Lau, H.Y. (2020). A study of cybersickness and sensory conflict theory using a motion-coupled virtual reality system. *Displays* 61, 101922.
- Nie, G.-Y., Duh, H.B.-L., Liu, Y., and Wang, Y. (2019). Analysis on mitigation of visually induced motion sickness by applying dynamical blurring on a user's retina. *IEEE transactions on visualization and computer graphics* 26, 2535-2545.
- Nooij, S.A., Bockisch, C.J., Bühlhoff, H.H., and Straumann, D. (2021). Beyond sensory conflict: The role of beliefs and perception in motion sickness. *PLoS One* 16, e0245295.
- Oliva, R., Beacco, A., Navarro, X., and Slater, M. (2022). QuickVR: A Standard Library for Virtual Embodiment in Unity. *Frontiers in Virtual Reality* 3:937191. doi.org/10.3389/frvir.2022.937191
- Purves, D., Augustine, G., and Fitzpatrick, D. (2001). Anatomical Distribution of Rods and Cones, editors. *Neuroscience. 2nd edition. Sunderland (MA): Sinauer Associates.*
- Reason, J.T., and Brand, J.J. (1975). *Motion sickness*. Academic press.
- Riccio, G.E., and Stoffregen, T.A. (1991). An ecological theory of motion sickness and postural instability. *Ecological psychology* 3, 195-240.
- Saredakis, D., Szpak, A., Birckhead, B., Keage, H.a.D., Rizzo, A., and Loetscher, T. (2020). Factors Associated With Virtual Reality Sickness in Head-Mounted Displays: A Systematic Review and Meta-Analysis. *Front Hum Neurosci* 14, 96. 10.3389/fnhum.2020.00096
- Sinitski, E.H., Thompson, A., Godsell, P., Honey, J., and Besemann, M. (2018). Postural stability and simulator sickness after walking on a treadmill in a virtual environment with a curved display. *Displays* 52, 1-7.
- Slater, M., and Steed, A. (2000). A Virtual Presence Counter. *Presence: Teleoperators and Virtual Environments* 9, 413-434. 10.1162/105474600566925
- Stanney, K.M., and Kennedy, R.S. (2009). "Simulation sickness," in *Human factors in simulation and training*, eds. D.A. Vicenzi, J.A. Wise, M. Mouloua & P.A. Hancock. (Boca Raton, Florida: CRC Press), 117-127.

- Vehtari, A., and Gelman, A. (2014). WAIC and cross-validation in Stan. Submitted. *City*.
- Warwick-Evans, L., and Beaumont, S. (1995). An experimental evaluation of sensory conflict versus postural control theories of motion sickness. *Ecological Psychology* 7, 163-179.
- Warwick-Evans, L., Symons, N., Fitch, T., and Burrows, L. (1998). Evaluating sensory conflict and postural instability. Theories of motion sickness. *Brain research bulletin* 47, 465-469.
- Widdowson, C., Becerra, I., Merrill, C., Wang, R.F., and Lavelle, S. (2021). Assessing postural instability and cybersickness through linear and angular displacement. *Human factors* 63, 296-311.